Mechanism and reduction of temporal image sticking in ac plasma display panel

Choon-Sang Park and Heung-Sik Tae[a)]
School of Electrical Engineering and Computer Science, Kyungpook National University, Daegu 702-701, Republic of Korea

(Received 28 September 2009; accepted 26 December 2009; published online 28 January 2010)

It is found that temporal image sticking in ac plasma display panels (PDPs) is predominantly induced by organic impurities, such as C_xH_y, on the MgO surface. The vacuum ultraviolet produced during a short sustain discharge dissociates these organic impurities, such as C_xH_y, into C and H, where the latter then combines with the O from the MgO surface, resulting in the production of chemical compounds, including H_2O, that lower the luminance by hindering the visible conversion of the phosphor layer. Thus, according to this mechanism, minimizing the residual organic impurities, such as C_xH_y, on the MgO surface is a key factor for removing temporal image sticking. Therefore, to reduce the residual impurity level on the MgO layer of a 50 in. full-high definition (HD) ac-PDP with an He (35%)-Xe (11%) content, the MgO layer is given rf-plasma treatment using various gases, and the experimental results show that Ar plasma treatment was most effective in eliminating the residual impurities on the MgO layer and thereby improving the temporal image sticking. © *2010 American Institute of Physics*. [doi:10.1063/1.3294629]

As even a short sustain discharge can induce image retention or temporal image sticking in current ac plasma display panels (PDPs),[1–10] this problem needs to be solved urgently in order to realize a high-quality PDP. However, the temporal image sticking phenomenon is still not clearly understood.

Accordingly, this letter presents in detail the mechanism responsible for inducing temporal image sticking. Based on this mechanism, an effective method is then proposed to reduce temporal image sticking. Since residual organic impurities, such as C_xH_y, on the MgO surface are implicated as the main source for inducing the temporal image sticking phenomenon, these residual organic impurities are eliminated by treating the MgO surfaces of the PDP for 30 min. with Ar or O_2 rf-plasma. In particular, several different gases are used for the rf-plasma treatment to determine which is the most effective for eliminating the residual organic impurities on the MgO surface.

Figure 1 shows a schematic model of the mechanism responsible for inducing temporal image sticking in an ac plasma display panel. As shown in Fig. 1, residual organic impurities, such as C_xH_y, remain on the MgO surface. This residual organic matter (C_xH_y) is dissociated into C and H by the VUV, electrons, or ions produced by an iterant sustain discharge, and the dissociated hydrogen atoms then react with the oxygen supplied from the MgO surface as a result of ion bombardment. Finally, a hydrate, such as H_2O, is produced, which has a deteriorating effect on the visible conversion of the phosphor layer when absorbed.[11–13] The resultant luminance is also lowered due to the aggravated visible conversion rate of the phosphor layer, which is called "temporal image sticking." Consequently, based on this mechanism, the presence of residual organic impurities, such as C_xH_y, on the MgO surface plays a significant role in aggravating the visible conversion of the phosphor layer.

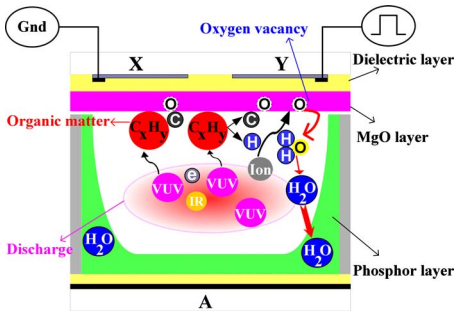

FIG. 1. (Color online) Mechanism inducing temporal image sticking in ac plasma display panel.

Table I shows the changes in the disappearing time of temporal image sticking for 42 in. PDPs with different Xe contents, where a longer disappearing time means more severe temporal image sticking. As shown in Table I, the temporal image sticking became more severe in proportion to an increase in the Xe%. An increase in the Xe% means a decrease in the Ne%. With a higher Xe%, more VUV was produced, whereas with a lower Ne%, the sputter yield decreased. The production of the temporal image sticking strongly depends on which factor (i.e., an increase in VUV intensity or a decrease in sputter yield) has more significant influence on the dissociation of the residual organic impuri-

TABLE I. Changes in disappearing time of temporal image sticking with full-white background before and after 1 min. iterant sustain discharge in 42 inch HD panels with various Xe gas contents.

Panel	Disappearing time (sec.)
Xe 11%-He 51%-Ne	48
Xe 15%-He 51%-Ne	75
Xe 20%-He 51%-Ne	190

[a)]Electronic mail: hstae@ee.knu.ac.kr.

TABLE II. Specifications of 50 in. full-HD ac-PDPs used in this study.

Front Panel		Rear Panel	
ITO width	210 μm	Barrier rib width	50 μm
ITO gap	70 μm	Barrier rib height	120 μm
Bus width	70 μm	Address width	85 μm
Pixel pitch		576 μm$\times$576 μm	
Gas chemistry		Ne-Xe (11%)-He (35%)	
Gas pressure		430 Torr	
Barrier rib type		Closed rib	

ties on the MgO layer. Of the two factors, the result in Table I confirmed that an increase in VUV intensity facilitated the dissociation of the organic impurities, such as C_xH_y, on the MgO layer. In view of luminous efficacies, the increase in the Xe% is necessary, meaning that if the organic impurities exist on the MgO layer, the severeness of the temporal image sticking can be unavoidable under a high Xe% gas condition. Accordingly, to minimize the temporal image sticking in spite of increase in the Xe%, it is very important to eliminate the amount of the organic impurities on the MgO layer. Thus, to reduce the residual impurity level on the MgO layer in a 50 in. full-HD ac-PDP, the MgO layer is given rf-plasma treatment using several different gases. In particular, the rf-plasma treatment used the two kinds of plasma gas composition, $O_2>$Ar [O_2: 201 sccm and Ar: 22 sccm (SCCM denotes cubic centimeter per minute at STP)] and Ar (240 sccm), to investigate which gas in the rf-plasma treatment would be most effective in reducing the temporal image sticking of the ac-PDP. The rf (13.56 MHz) input power and process time for the plasma treatment were 4 kW and 30 min, respectively.[14] The frequency for the sustain period was 200 kHz, and the sustain voltage was 205 V.[14] The detailed panel specifications were exactly the same as those listed in Table II, except for the plasma treatment gas composition.

Figure 2 shows the changes in the organic matter on the MgO surface of the 50 in. test panels prepared using rf-plasma treatment with various gas compositions. The organic impurities on the MgO surface were measured by using the time of flight secondary ion mass spectrometry (TOF-SIMS) analysis. The TOF-SIMS measured the total count of the secondary ion emitted from the MgO surface when the MgO surface was struck for 100 s by the primary Bi ions from the ion gun with 25 keV. The primary ion beam energy was 1 pA, and the measurement area was 150$\times$150 μm^2. The electron gun was used not to charge the dielectric MgO surface by the secondary ion when it was sputtered during measurement. As shown in Fig. 2, the $O_2>$Ar plasma treatment resulted in almost the same organic matter on the MgO surface as with the nonplasma treatment (refer Fig. 4(a) panel). However, the Ar plasma treatment reduced the organic matter on the MgO surface when compared with the nonplasma treatment and $O_2>$Ar plasma treatment.

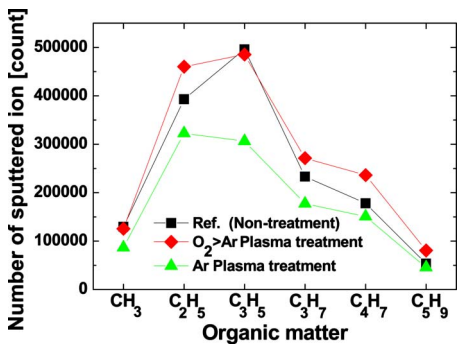

FIG. 2. (Color online) Comparison of organic matter (C_xH_y) on MgO surface based on TOF-SIMS analysis of 50 in. full-HD panels prepared using rf-plasma treatment with various gas compositions.

TABLE III. Comparison of roughness of MgO surface based on AFM analysis of 50 in. full-HD panels prepared using rf-plasma treatment with various gas compositions.

Panel	Roughness [Rrms, Å]
Refer Fig. 4(a) (nonplasma treatment)	136.7
$O_2>$Ar Plasma treatment	98.3
Ar Plasma treatment	16.1

Table III shows the changes in the roughness of the MgO surface based on an AFM analysis of the 50 in. test panels prepared using rf-plasma treatment with various plasma gas compositions. As shown in Table III, the $O_2>$Ar plasma treatment produced a slight reduction in the roughness of the MgO surface when compared with the nonplasma treatment. However, the Ar plasma treatment considerably reduced the roughness of the MgO layer when compared with the nonplasma treatment, implying that the physical sputtering was dominantly produced by the Ar plasma treatment. Accordingly, Fig. 2 and Table III illustrated that the physical sputtering of the Ar rf-plasma treatment was more effective in reducing the organic matter on the MgO surface than the chemical sputtering of the O_2 rf-plasma.

Figure 3 shows the changes in the luminance difference before and after a sustain discharge and the disappearing time of temporal image sticking with a full-white background after a 5 min. iterant sustain discharge. The test panels were also 50 inch full-HD panels prepared using rf-plasma treatment with various gas compositions. In Fig. 3, the luminance after sustain discharge was decreased. As shown in Fig. 3, the $O_2>$Ar plasma treatment produced almost the same luminance difference and disappearing time as the nonplasma treatment. However, the Ar plasma treatment considerably reduced the display luminance difference, ΔL, and disappearing time to 3.1 cd/m^2 and 15 s, respectively

Figure 4 shows the changes in the infrared (IR: 828 nm) emissions in the discharge region with a full-white back-

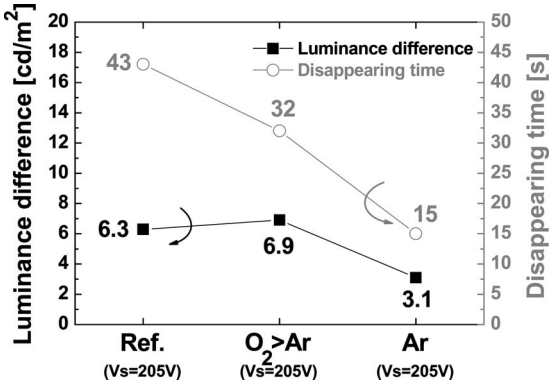

FIG. 3. Comparison of luminance difference and disappearing time of temporal image sticking with full-white background before and after 5 min. iterant sustain discharge in 50 inch full-HD panels prepared using rf-plasma treatment with various gas compositions.

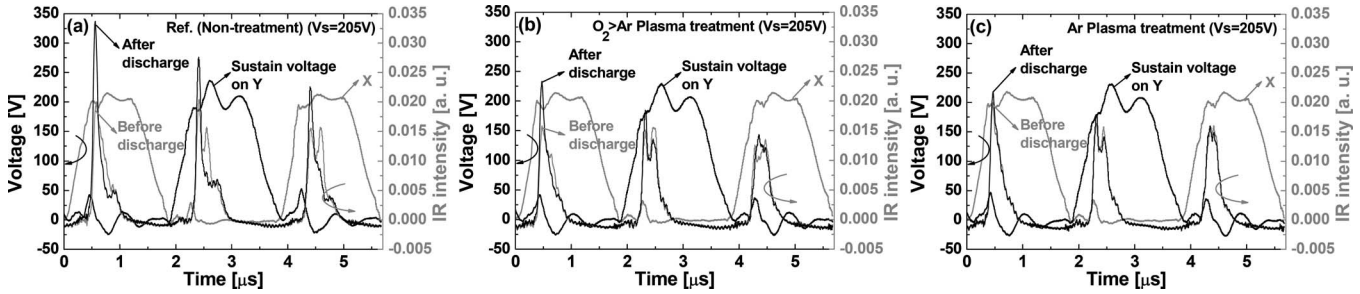

FIG. 4. Changes in IR (828 nm) emissions measured from discharge region with full-white background before and after 5 min. iterant sustain discharge in 50 inch full-HD panels prepared using rf-plasma treatment with various gas compositions: (a) nonplasma treatment, (b) $O_2>$Ar plasma treatment, and (c) Ar plasma treatment.

ground measured before and after a 5-min. iterant sustain discharge in the 50-inch full-HD panels prepared using rf-plasma treatment with various gas compositions. For O_2 or Ar rf-plasma treatment, the IR emissions were slightly decreased compared to that for nonplasma treatment. However, in case of both non and $O_2>$Ar plasma treatments, the IR peaks after sustain discharge were intensified compared to that before sustain discharge, whereas the luminance after sustain discharge was deteriorated. This confirmed that the deterioration in the luminance was induced only by the change in the visible conversion of phosphors. With the Ar plasma treatment, however, the IR emissions in the discharge region were almost the same before and after a discharge. Furthermore, the Ar plasma treatment induced a reduced firing voltage due to an enhanced secondary electron coefficient of the MgO layer [not shown here].[14] Thus, the Ar plasma treatment facilitated a lower sustain voltage that was more effective for reducing temporal image sticking. As a result, the display luminance difference, ΔL, measured at the lower sustain voltage of 192 V, was considerably reduced to 1.5 cd/m^2, meaning no temporal image sticking.

In summary, temporal image sticking was shown to be strongly related to the presence of organic matter, such as C_xH_y, on the MgO surface, however, these organic impurities were effectively eliminated by treating the MgO surface with Ar rf-plasma. Consequently, Ar rf-plasma treatment of the MgO surface is an effective method for reducing temporal image sticking.

This work was supported in part by the IT R&D program of MKE/KEIT [2009-5-009-01, Development of Eco-friendly 50" Quadro Full HD PDP Technology] and in part by the Brain Korea 21 (BK21).

[1]H.-S. Tae, J.-W. Han, S.-H. Jang, B.-N. Kim, B. J. Shin, B.-G. Cho, and S.-I. Chien, IEEE Trans. Plasma Sci. **32**, 2189 (2004).
[2]H.-S. Tae, C.-S. Park, B.-G. Cho, J.-W. Han, B. J. Shin, S.-I. Chien, and D. H. Lee, IEEE Trans. Plasma Sci. **34**, 996 (2006).
[3]J.-W. Han, H.-S. Tae, B. J. Shin, S.-I. Chien, and D. H. Lee, IEEE Trans. Plasma Sci. **34**, 324 (2006).
[4]C.-S. Park, B.-G. Cho, and H.-S. Tae, J. Inf. Disp. **9**, 39 (2008).
[5]C.-S. Park, H.-S. Tae, Y.-K. Kwon, and E. G. Heo, IEEE Trans. Electron Devices **54**, 1315 (2007).
[6]C.-S. Park, H.-S. Tae, Y.-K. Kwon, and E. G. Heo, IEEE Trans. Plasma Sci. **35**, 1511 (2007).
[7]C.-S. Park, H.-S. Tae, Y.-K. Kwon, E. G. Heo, and B.-H. Lee, IEEE Trans. Electron Devices **55**, 1345 (2008).
[8]C.-S. Park and H.-S. Tae, IEICE Trans. Electron. **92-C**, 161 (2009).
[9]C.-S. Park and H.-S. Tae, Appl. Opt. **48**, F76 (2009).
[10]C.-S. Park, H.-S. Tae, Y.-K. Kwon, and E. G. Heo, Mol. Cryst. Liq. Cryst. **499**, 213 (2009).
[11]B. Moine and G. Bizarri, J. Soc. Inf. Disp. **16**, 55 (2008).
[12]T. Onimaru, S. Fukuta, T. Misawa, K. Sakita, and K. Betsui, IEICE Trans. Electronics **86-C**, 2253 (2003).
[13]K. C. Mishra, M. Raukas, G. Marking, P. Chen, and P. Boolchand, J. Electrochem. Soc. **152**, H183 (2005).
[14]C.-S. Park, H.-S. Tae, B.-K. Park, E.-Y. Jung, and J.-C. Ahn, *Digest of Technical Papers of 2009 Society for Information Display International Symposium* (Society for Information Display, San Antonio, 2009), p. 363.